Applied Physics A (2025) 131:852
https://doi.org/10.1007/s00339-025-09031-7

Applied Physics A
Materials Science & Processing

Pristine SnO_2 thin films: origins of high Curie temperature

Nguyen Sy Pham[1] · Nguyen Que Huong[2] · Petr Pazourek[1] · Mojmir Meduna[1] · Ondrej Caha[1] · Nguyen Hoa Hong[1]

Received: 5 August 2025 / Accepted: 2 October 2025

Abstract
We investigate the origin of ferromagnetism (FM) and the exceptionally high Curie temperature (T_C) in undoped SnO_2 films. Ultra-thin SnO_2 films were found to exhibit significant FM, while thicker films show a diamagnetic behavior. Structural and chemical analyses reveal a variation in oxygen vacancy concentrations between thin and thick films. Notably, an exceptionally high T_C exceeding 800 K is observed for the first time. XPS and XAS analyses reveal the presence of oxygen and tin vacancies, which might play a crucial role in the observed magnetism. Theoretically, it was supposed that oxygen vacancies play a crucial role in the FM of SnO_2 films. However, the experimentally observed T_C surpasses the predicted 505 K, suggesting additional contributing factors. This suggests that both oxygen and tin defects might contribute to the total magnetic moment. The findings highlight the key role of defect-induced magnetism in SnO_2 thin films and provide insights into the fundamental mechanism driving high- T_C FM in undoped oxide semiconductors.

Keywords Surface-related ferromagnetism · High T_C · Low dimensionality · Spintronics

1 Introduction

Having both charges and spins in one compound, and being considered as potential candidates for spintronic applications, magnetic semiconducting oxides have garnered significant attention. The observation of the room temperature ferromagnetism (FM) in undoped semiconducting oxides in nanostructures [1–5] has been regarded as a remarkable phenomenon in the field of magnetism. The question of the origin of the observed FM has been raised. Since these materials lack transition-metal (TM) doping, the observed FM cannot be attributed to double-exchange (DE) interactions [1–7]. Instead, oxygen vacancies and defects are believed to be the primary cause of the ferromagnetic behavior of pristine semiconducting oxides. Supporting this assumption, post-annealing samples in an oxygen-rich environment significantly reduced their magnetic ordering [2, 3].

A theoretical study conducted a few years ago suggested that in TiO_2 and SnO_2, FM arises from oxygen vacancies [8]. It was demonstrated that vacancy sites in these oxides induce spin splitting with a high-spin state, and the exchange interaction between the electrons surrounding the vacancy and the local symmetry field results in a ferromagnetic ground state [8]. The nanoscale size of these materials, along with quantum confinement effects, plays a crucial role in their magnetic properties [8, 9]. Room-temperature FM has been reported in pristine SnO_2 films [3, 7] as well as in SnO_2 nanoparticles [5].

X-ray absorption spectroscopy (XAS) measurements indicate that surface-related defects exhibit a magnetic triplet ground state, whereas the bulk SnO_2 ground state remains in a non-magnetic singlet state [6]. Other studies on SnO_2 nanoparticles with special oxygen treatments suggest that FM is predominantly a surface effect [10, 11]. In research involving TM, multiple studies have shown that neither the type of dopant nor its concentration significantly affects the Curie temperature (T_C), leading to the conclusion that TM doping is not the primary cause of FM in these materials [12].

Recent studies on SnO_2 films suggest that their FM behavior is inherently two-dimensional (2D), reinforcing

✉ Nguyen Hoa Hong
hong.nguyen@mail.muni.cz

[1] Department of Condensed Matter Physics, Faculty of Science, Masaryk University, Kotlářská 2, Brno 61137, Czechia

[2] Department of Mathematics and Physics, Marshall University, One John Marshall Drive, Huntington 25755, WV, US

Published online: 14 October 2025

the hypothesis that it is surface-related [13]. Regarding the T_C of diluted magnetic semiconducting oxides, values of approximately 880 K have been reported for TiO_2 films [4], however, to date, no T_C value has been reported for undoped SnO_2 films, regardless of the fabrication method used.

In this study, we will examine the T_C of SnO_2 films and related issues. Additionally, we will discuss the origin of FM in ultra-thin SnO_2 films and compare our findings with theoretical predictions.

2 Experiment

SnO_2 films were deposited using a Pulsed-Laser Deposition (PLD) system (KrF, 248 nm) from a SnO_2 ceramic target onto (100) $LaAlO_3$ (LAO) substrates. The deposition was performed with an energy density of 2 J/cm² and a repetition rate of 10 Hz. The optimized growth conditions included a substrate temperature of 650 °C, an oxygen pressure of 0.01 mbar, and an O_2:Ar flow ratio of 50:50. The typical film thickness ranged from 50 nm to 340 nm. All SnO_2 films appeared shiny and highly transparent. Structural characterization was conducted using X-ray diffractions (XRD) at room temperature. Magnetic moment (*M*) as a function of the magnetic field (*H*) (0 to 0.5 T) and temperature (*T*) (50 K to 900 K) was measured using a VSM magnetometer. X-ray Photoelectron Spectroscopy (XPS) was used at room temperature to determine the chemical states. The magnetic field was applied both parallel and perpendicular to the film plane. The thickness of typical films was measured using a NIR-UV spectroscopic ellipsometer J.A. Woollam V-VASE in the wavelength range of 400 to 1000 nm, with the Cauchy method used for thickness determination. Film morphology and chemical composition were analyzed using Scanning Electron Microscopy (SEM TESCAN LYRA 3) and energy-dispersive spectroscopy (Bruker XFlash 5010), with SEM images captured at a 5 kV accelerating voltage. Further structural investigations of films with varying thicknesses were carried out using X-ray Reflectivity (XRR) and X-ray Absorption Spectroscopy (XAS) at room temperature, conducted at beamline PM3 of the BESSY II Synchrotron center. Additionally, the drain signal was measured at an incidence angle of 4.5°.

3 Theory

We use the tight-binding or linear combination of molecular orbitals (LCMO) method [8] to explore the possibility of FM and T_C in SnO_2 due to oxygen vacancies in 2D configurations. FM and high T_C have been observed only in thin films, not in bulk materials, suggesting that the 2D configuration plays a crucial role.

The Sn atom has an electronic configuration of $[4d^{10}5s^25p^2]$, where the 2 5s- and 2 5p- electrons participate in bonding with oxygen, resulting in a Sn^{4+} ion with a closed-shell $[Pd]4d^{10}$ configuration, with no unpaired electrons. In the rutile tetragonal local symmetry D_{4h} of SnO_2 molecule, each two of Sn atoms are surrounded by six oxygen atoms [14]. If an oxygen vacancy occurs, the 2p electrons lose their bonding but remain in the shell, forming a p^2 impurity center. The exchange interaction among these p-electrons, as well as their interaction with the molecular orbital in the local tetragonal symmetry, alters the energy states, increase the energy and modifies the magnetic moment, eventually, affecting T_C.

The two p-electrons, each occupying a two-fold degenerate e-orbital, couple with each other to form a configuration represented by the product decomposition $E \times E = A_1 + A_2 + E$ through the reduction process [15, 16]. The wave functions of the two coupling E-orbitals could be written as.

$$|e^2,\ ^1A_1, M_s = 0\rangle,\ |e^2,\ ^3A_2,\ M_S = 1\rangle, |e^2, ^3A_2, M_s = 0\rangle, |e^2,\ ^3A_2, M_S = -1\rangle$$

for $^1A_1$and $^3A_2$orbitals; and

$$|e^2, ^1Eu, M_s = 0\rangle, |\ e^2, ^1Ev, M_s = 0\rangle$$

for ^1E orbital, corresponding to $M_s = 0$ and $M_s = 1$, while satisfying the Pauli exclusion principle.

Since oxygen is a four-valence anion, the absence of one oxygen atom creates four additional electrons in the impurity band. Being around a vacancy center, an electron would interact with the impurity band through Coulomb and exchange interaction, given by

$$H_{ex} = -JS_I s_e$$

where S_J is the total spin of the impurity configuration, s_e is the spin of the electron, and J is the exchange matrix element, which consists of radial and angular components.

To account for the thin-film configuration, we impose strong confinement of wavefunctions along the z-axis. This confinement localizes the electrons further, increasing their sensitivity to local symmetry and enhancing the exchange interaction.

Using the mean-field approximation

$$k_B T_c = \frac{2}{3}\sum_{ij} J_{ij}$$

including the exchange integrals at oxygen vacancy sites, we obtained $k_B T_c$ around 6.95×10^{-21}, corresponding to the T_C of about 505 K.

4 Results and discussions

X-ray diffraction (XRD) patterns of our SnO_2 films and a bare $LaAlO_3$ substrate are shown in Fig. 1. SnO_2 films with different thicknesses all exhibit a single-phase structure with distinct (200) and (101) peaks in the diffractograms. All the diffraction peaks including (101), (200) can be attributed to tetragonal rutile structure of SnO_2 and well matches with JCPDS card No. 41–1445 [17]. The presence of these peaks is significant and will be discussed later in the context of verifying the magnetic anisotropy of the SnO_2 films. The morphology of a typical SnO_2 thin film is displayed in Fig. 2, demonstrating its high homogeneity. Additionally, EDS mapping (Fig. 2b–d) reveals a uniform distribution of O and Sn elements across the film. Further structural investigations of the SnO_2 films were conducted using XRR measurements. To enable XAS measurements, SnO_2 films of varying thicknesses were coated with a thin carbon layer of a few nanometers. In our analysis, d_{SnO2} represents the thickness of the SnO_2 layer, while d_C denotes the thickness of the carbon coating, both obtained from simulations using GenX software [18]. The roughness parameter (σ) corresponds to the highest interface roughness value determined from these simulations.

The XAS measurements were performed at 280 K, close to the Sn absorption edge (484.9 eV), using X-rays with an energy of 480 eV. As seen in Fig. 3, when simulated with XRR data, the 50 nm- and 100 nm-thick SnO_2 films exhibit a thickness that is slightly smaller than the objective thickness. However, when accounting for the carbon coating, the total thickness closely matches each other. The SnO_2 films are generally rough, with the roughness determined to be (2.8 ± 0.4) nm for the 100 nm-thick film and (2.5 ± 0.5) nm for the 50 nm-thick film.

The *M(H)* curves of magnetization versus magnetic field for the 74 nm-thick SnO_2 film are shown in Fig. 4(a). The magnetic field was applied either parallel or perpendicular to the film plane. The inserts show the magnified views of these curves, allowing a clearer observation of coercivity (H_C). Our SnO_2 thin films exhibit soft magnetic behavior with a small H_C. The 74 nm-thick SnO_2 film demonstrates a remarkably large saturated magnetization (M_s), i.e. almost an order of magnitude greater than the highest previously reported value for SnO_2 [3]. Comparing with the same filmed being measure a year earlier, M_s decreased by only 20% over a one-year time, indicating minimal aging effects and suggesting that the films are durable enough for device applications. Interestingly, despite the difference in M_s when measured in the perpendicular configuration, the film maintains ferromagnetic above room temperature. This observation aligns with some theoretical modeling, which suggests that oxygen and tin defects may induce ferromagnetic ordering along certain axes while promoting a mixed ferromagnetic-ferrimagnetic state along others [13]. This

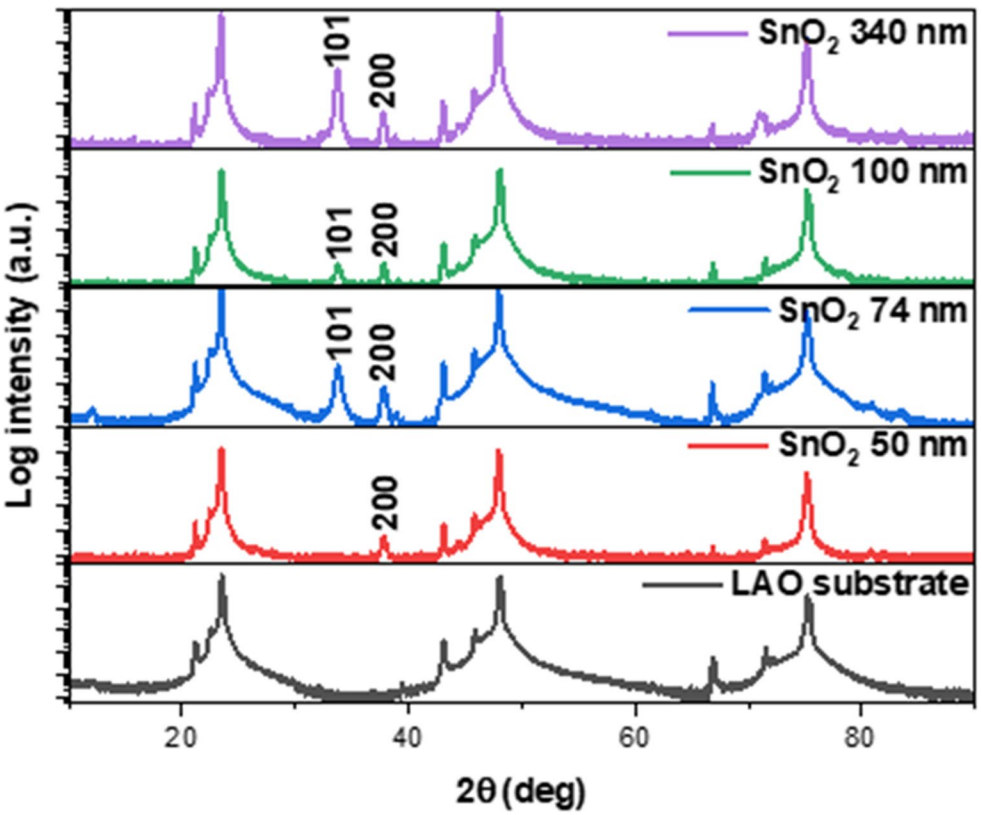

Fig. 1 XRD patterns of SnO_2films with different thicknesses deposited on $LaAlO_3$substrate and of a bare $LaAlO_3$substrate

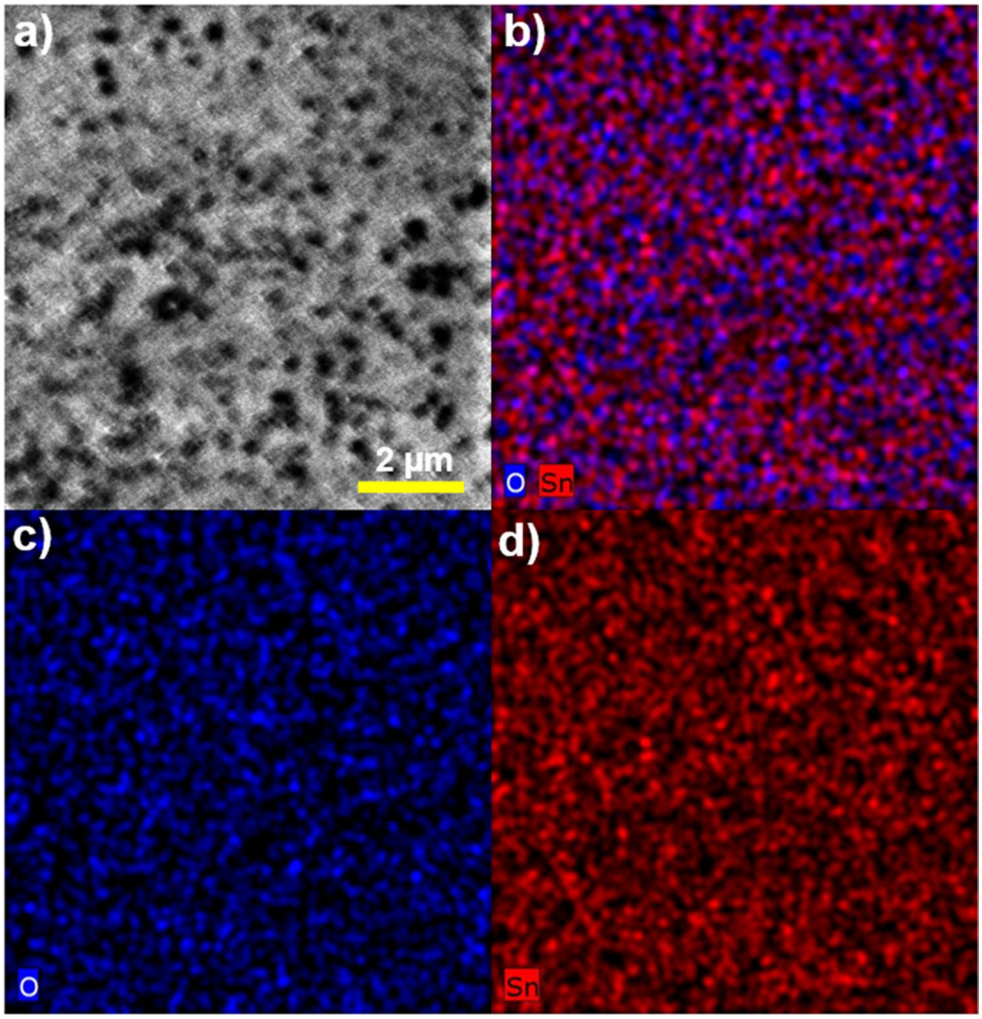

Fig. 2 **a**) SEM image of the 74 nm-thick SnO_2 film; **b**) general color mapping result of SnO_2 film; **c**) O color mapping; **d**) Sn color mapping

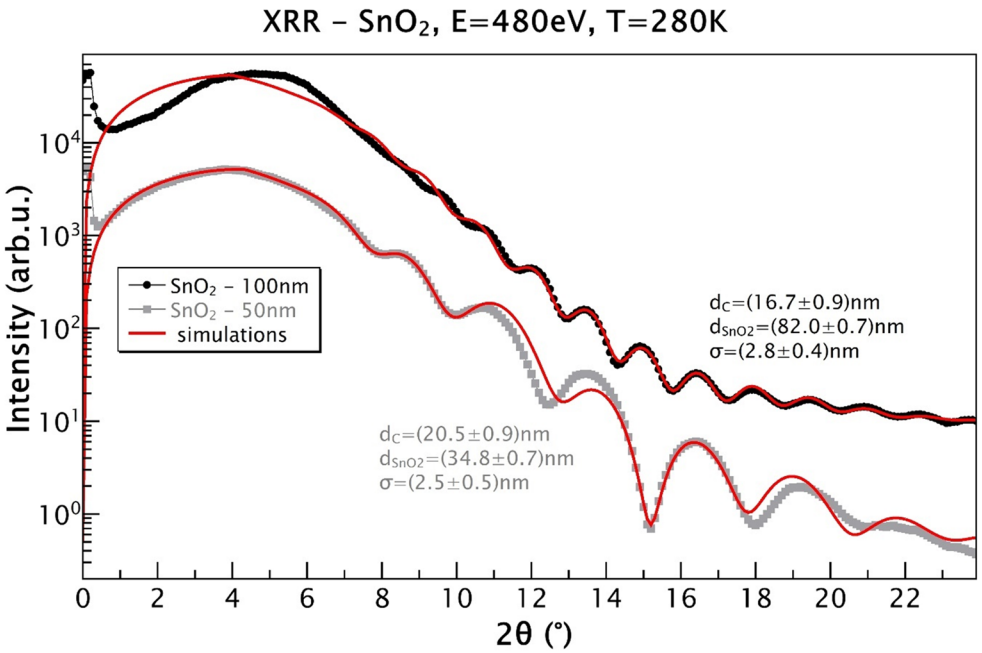

Fig. 3 XRR data and simulations for SnO_2 films with nominal thicknesses of 50-100 nm covered by C. d_{SnO2}denotes the thickness of the SnO_2 layer ; $d_C$represents the C top layer thickness; the σ represents the highest roughness value of the interfaces obtained from simulations

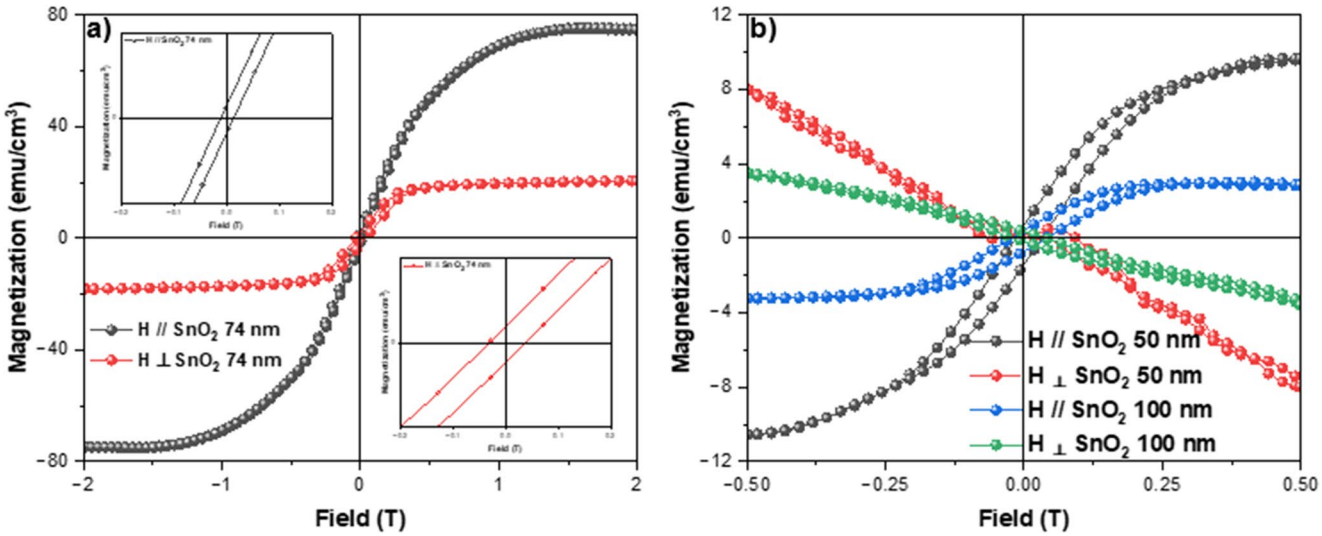

Fig. 4 Field dependence of magnetization taken at 300 K for (**a**) the 74 nm- SnO_2 film with magnetic field applied parallel and perpendicular to the film plane. The inserts are zooms of the two M-H curves to reveal H_C; and (**b**) for the 50 and 100 nm-thick SnO_2 films with magnetic field applied parallel and perpendicular to the film plane

characteristic is also evident in the *M-H* data for films of varying thicknesses, as shown in Fig. 4(b). Table 1 lists the M_s values for all studied films, revealing that the 50 nm-thick film exhibits an M_s of approximately 9 emu/cm³, lower than that of the 74 nm-thick film, while the M_s of the 100 nm-thick film is also smaller. If the total magnetic moment of SnO_2 depends on the precise locations of O and Sn defects, as well as their relative distances, it can explain why magnetization is not dependent linearly on the film thickness. The thin layers near to the surface primarily dictate the magnetic properties of SnO_2, and there exists a critical line distinguishing ferromagnetic and ferrimagnetic behavior. In 50 nm -and 100 nm- thick films, a diamagnetic behavior was detected when the magnetic field applied perpendicular to the film's plane, confirming the existence of anisotropy in this family of materials, and it well suggests that the FM in this films most probably has the origin from defects and/or vacancies. The FM in SnO_2 films is well in-plane.

Table 1 Saturated magnetization for SnO_2 films with different thicknesses

Thickness (nm)	50	74	100	340
Saturated magnetization (emu/cm³)	**9**	**78**	**3**	**<0**

The XPS spectra for O1s of 74 nm - thick SnO_2 film and the 340 nm-thick SnO_2 film are shown in Fig. 5. While XPS

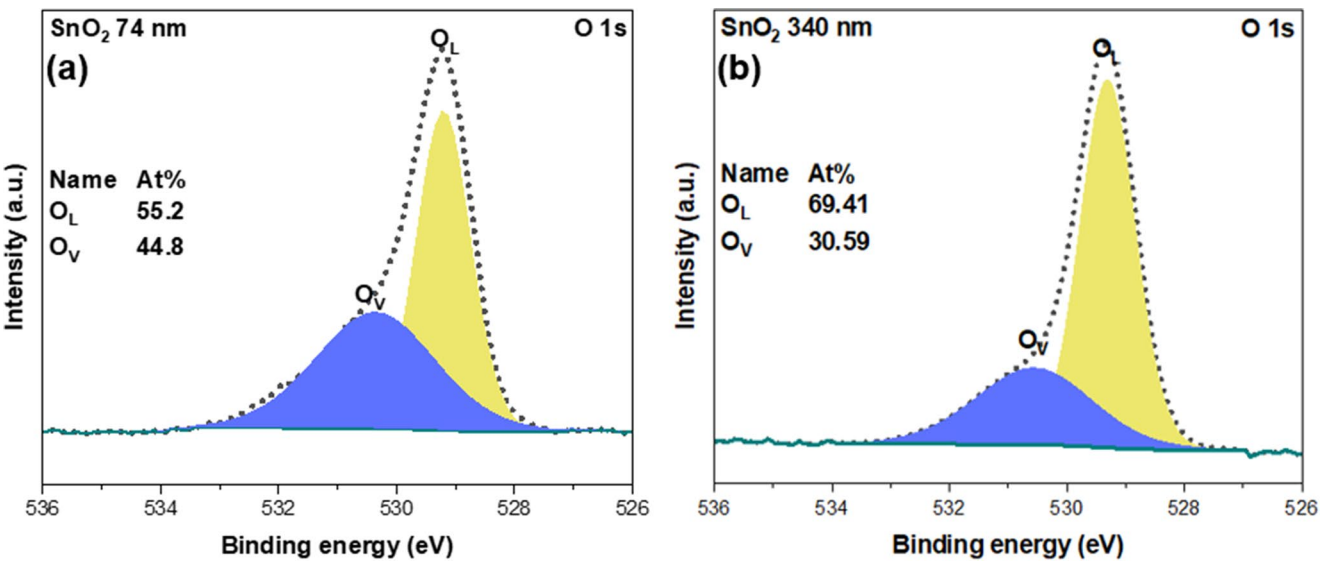

Fig. 5 Analysis of chemical states from high resolution XPS spectra for (**a**) O1s for the 74 nm-thick SnO_2 film; (**b**) O1s general for the 340 nm-thick

mostly provides surface-sensitive data, it remains relevant since magnetism in SnO_2 films is largely surface-related, and the XPS data still can reflect well the concerned properties of the film.

Figure 5(a) shows a broad peak in the O spectrum of the 74 nm-thick SnO_2 film, which can be curve-fitted into two peaks with binding energies of approximately 529.2 eV and 530.5 eV respectively. The former represents lattice oxygen (O_L) in the SnO_2 crystal structure, while the latter corresponds to oxygen vacancies (O_V) on the film surface. Similar features have been reported for O vacancies in SnO_2 [19]. To compare how oxygen vacancies can be different for films with different thicknesses, XPS measurements were also conducted on the diamagnetic 340 nm-thick SnO_2 film, as shown in Fig. 5(b). Notably, the ferromagnetic 74 nm-thick film exhibits a higher concentration of oxygen vacancies compared to the diamagnetic 340 nm-thick film, as evident from Fig. 6. Additionally, the chemical state of Sn in the 74 nm-thick SnO_2 thin film was further analyzed using XPS (Fig. 6). The deconvolutions of the Sn $3d_{3/2}$ and Sn $3d_{5/2}$ peaks reveal four distinct peaks: those at 495.26 eV and 486.85 eV correspond to Sn^{4+} states, while the peaks at 493.39 eV and 484.76 eV are attributed to Sn^{2+} states [20] The material composition is notably dominated by Sn^{4+} states [21].

XAS data for SnO_2 thin films are shown in Fig. 7. The absorption spectra at the O edge and Sn edge are shown in Fig. 7(a) and Fig. 7(b), respectively. Certain differences are observed between the spectra of the 50 nm-thick and 100 nm-thick films. In general, quantum confinement effects in very thin films can induce shifts in the absorption edge. Additionally, surface and interface states may significantly influence electronic transitions in thinner films. The 50 nm-thick film is likely to have a higher density of defects compared to the 100 nm-thick film, which can lead to modifications in the absorption edge. Such shifts shift in the absorption edge of films with different thicknesses indicate variations in the bandgap energy, as reported in Ref [6]. Differences in the absorption spectra at both the O and Sn edges have been observed, confirming that the thin and thick films exhibit different defect densities whether due to O or Sn vacancies, resulting in variations in their bandgap energies. The Sn-$M_{4,5}$ absorption edges ($3d_{3/2}$ and $3d_{5/2}$) display a characteristic double structure with a relative shift of 2.1 eV, corresponding to two oxidation states of Sn. This observation agrees well with the XPS analysis above (Fig. 6) and the corresponding magnetization data. The presence of Sn vacancies and defects is evidently linked to the reported magnetic moment in these films.

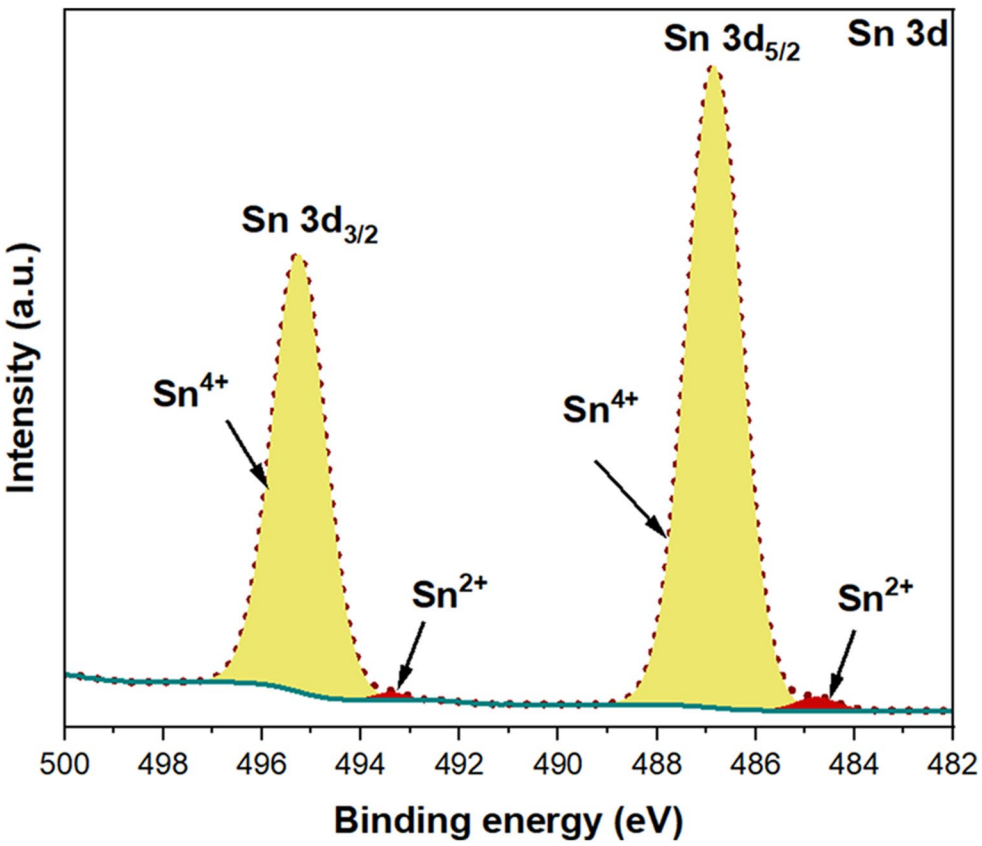

Fig. 6 XPS spectrum of the Sn $3d_{3/2}$ and Sn $3d_{5/2}$ peaks for the 74 nm-thick SnO_2 film

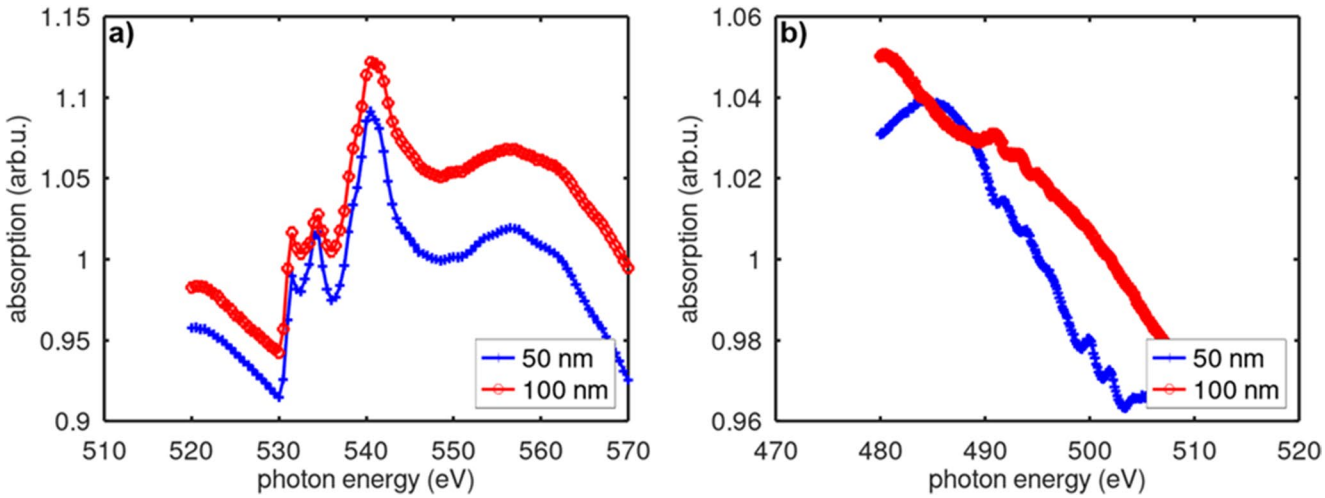

Fig. 7 Absorption spectra seen from **a**) O edge and **b**) Sn edge for 50 nm-thick and 100 nm-thick films of SnO_2

The magnetization versus temperature curve for the 74 nm-thick SnO_2 film, taken at 2 T, is shown in Fig. 8. Notably, an exceptionally high Curie temperature of 850 K is observed for the first time. The SnO_2 film transitions into a ferromagnetic phase at approximately 850 K, as indicated by the intersection of the $M(T)$ curve with the T-axis and maintains ferromagnetic for the whole range of temperature below 850 K. To determine T_C more precisely, the dM/dT vs. T plot is also inserted into Fig. 8. A distinct minimum at 818 K in this plot confirms the transition temperature of our SnO_2 film to the ferromagnetic phase at around 818 K. In discussions regarding diluted magnetic semiconductors, it has been well established that T_C is often independent of the type of dopant or doping concentration [12]. For undoped semiconducting oxides, also known as d^0 magnetism, where no 3d element doping is present (i.e. no DE interaction can occur), predicting T_C is particularly challenging. Theoretically, T_C can be evaluated as:

$$T_C = \frac{2J_e Z\,[s[s+1]]}{3k_B}\ [22],$$

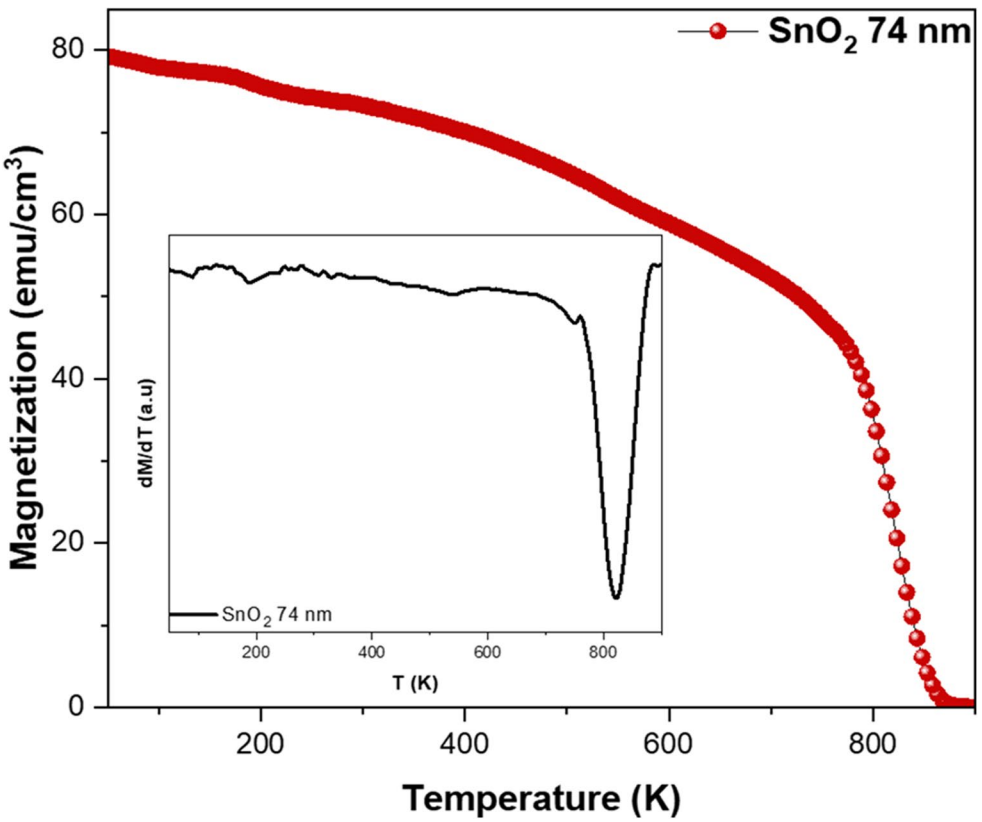

Fig. 8 Magnetization versus temperature taken at 2 T for the 74 nm-thick film (magnetic field was applied parallel to the film plane). The insert shows thedM/dT vs T curve

where J_e is the exchange integral, $S=1$ indicating a single electron, and Z is the number of nearest neighboring vacancies, and k_B is Boltzmann constant.

From our XPS data, for the 74 nm-thick-film, we estimate that each Sn atom has approximately three nearest neighboring oxygen vacancies, based the Sn/O and the O_L/O_V ratios. Using a Curie temperature T_C, of 818 K, spin S = 1, and Z = 3, we apply the above formula to estimate the exchange integral for SnO_2 as about 2.89×10^{-21} J. This value is of the same order of magnitude as the exchange integral of transition metals, which is typically around 10^{-21} J [23].

When considering only oxygen vacancies in a low-dimensional SnO_2 system, T_C was initially estimated to be 505 K, as mentioned earlier, theoretically. However, the experimentally observed T_C in our SnO_2 films is significantly higher (> 800 K). This discrepancy might be well explained by the presence of additional Sn vacancies/defects, which evidently exist in the laser ablated SnO_2 films as seen from our XPS and XAS data. These Sn-related defects might as well contribute to the overall magnetic interactions and the total magnetic moment, depending on their specific locations.

5 Conclusions

Ultra-thin SnO_2 films exhibit room-temperature ferromagnetism with a large magnetic moment, whereas thicker films display diamagnetic behavior like their bulk counterparts. This suggests the existence of a critical thickness required for ferromagnetism to emerge. Our study reveals distinct differences in O/Sn vacancies and defects between thin and thick films. An exceptionally high Curie temperature T_C exceeding 800 K was observed. Our theoretical calculations predict a high T_C, confirming that O/Sn vacancies and defects are the primary contributors to the magnetic moment in undoped SnO_2 films. The experimentally determined T_C is even higher than our theoretical estimate, suggesting that in addition to oxygen vacancies, Sn vacancies and defects play a crucial role in enhancing the total magnetic moment. Furthermore, the estimated exchange integral for SnO_2 films is of the same order as that found in transition metals, reinforcing the significance of defect-induced magnetism in these materials.

Supplementary Information The online version contains supplementary material available at https://doi.org/10.1007/s00339-025-09031-7.

Acknowledgements The authors acknowledge the financial support from the GACR (Project No. 22–21547 S) and the MEYS (Project CZ.02.01.01/00/22_008/0004572). N. Q. Huong would like to thank grant RCG23-007 (WVURC-MURC 23–049). We thank M. Kiaba and T. Q. Nhu for some technical support and A. Nebojsa for his help with thickness measurements. The CzechNanoLab Project No. LM2018110, funded by MEYS CR, is gratefully acknowledged for the financial support of the measurements and sample fabrication at the Central European Institute of Technology (CEITEC). We thank Synchrotron Bessy II for letting us use their facility and Torsten Kachel for assistance.

Author contributions N. H. Hong's role involves obtaining the funding, conceptualization, coordinating the work, supervising, interpreting data, and writing the articles. P. Pazourek made the films. N. S. Pham carried out the XRD, VSM, XPS, and SEM measurements and analyzed data and plotted figures. N. Q. Huong was in charge of the theoretical work and wrote her part in the article as well as editing the manuscript. M. Meduna and O. Caha performed the XRR and XAS measurements and analyzed related data. All authors checked and edited the final version of the manuscript.

Funding Open access publishing supported by the institutions participating in the CzechELib Transformative Agreement.

Data availability All data were included in the paper. Further details are available upon request made to the authors.

Declarations

Ethical approval Our experiments did not involve human tissues or similar matters.

Conflict of interest There are no conflicts of interest that exist for this manuscript.

References

1. M. Venkatesan, C.B. Fitzgerald, J.M. Coey, D. „ unexpected magnetism in a dielectric oxide. Nature. **430**, 630 (2004)
2. N.H. Hong, J. Sakai, N. Poirot, V. Brizé, Room-temperature ferromagnetism observed in undoped semiconducting and insulating oxide thin films. Phys. Rev. B **73**, 132404 (2006)
3. N.H. Hong, N. Poirot, Sakai, „ ferromagnetism observed in pristine thin films. Phys. Rev. B **77**, 33205 (2008)
4. S.D. Yoon, Y. Chen, A. Yang, T.L. Goodrich, X. Zuo, D.A. Arena, K. Ziemer, C. Vittoria, Oxygen-defect-induced magnetism to 880 K in semiconducting anatase TiO. Films. J. Phys. Condens. Matter. **18**, L355–L361 (2006)
5. A. Sundaresan, B. Bhagravi, N. Rangarajan, U. Siddesh, C.N. Rao, R., ferromagnetism as a universal feature of nanoparticles of the otherwise nonmagnetic oxides. Phys. Rev. B **74**(R), 161306 (2006)
6. G.S. Chang, J. Forrest, E.Z. Kurmaev, A.N. Morozovska, M.D. Glinchuk, J.A. McLeod, A. Moewes, T.P. Surkova, N.H. Hong,

Oxygen-vacancy-induced ferromagnetism in undoped SnO thin films. Phys. Rev. B. **85**, 165319 (2012)
7. J. Li, G. Bai, Y. Jiang, Y. Du, C. Wu, M. Yan, „Origin of room temperatture ferromagnetism in SnO_2 thin films. J. Mag Mag Mat. **426**, 545 (2017). https://doi.org/10.1016/j.jmmm.2016.12.002
8. N.Q. Huong, N.H. Hong, Ferromagnetism due to oxygen vacancies in low dimensional oxides. J. Mag Mag Mat. **534**, 167944 (2021)
9. O. Ciftja, Understanding electronic systems in semiconductor quantum dots. Phys. Scr. **88**, 058302 (2013). https://doi.org/10.1088/0031-8949/88/05/058302
10. A. Sundaresan, C.N.R. Rao, Ferromagnetism as a universal feature of inorganic nanoparticles. Nano Today **4**, 96 (2009)
11. A.T. Apostolov, I.N. Apostolova, S. Trimper, M. Wesselinova, Room temperature ferromagnetism in pure and ion-doped SnO. Nanopart. Mod. Phys. Lett. B. **31**, 1750351 (2017)
12. S.B. Ogale, „Dilute doping, defects, and ferromagnetism in metal oxide systems. Adv. Mater. **22**, 3125 (2010). https://doi.org/10.1002/adma.200903891
13. N.H. Hong, M. Friák, P. Pazourek, N.S. Pham, T.Q. Nhu, M. Kiaba, K. Gazdová, J. Pavlů, 2D nature of magnetic states at SnO_2 surfaces: a combined experimental and theoretical study. RSC Adv. **14**, 13583 (2024). https://doi.org/10.1039/d4ra00734d
14. S. Sugano, Y. Tanabe, H. Kamimura, *Multiplet of Transition Ions in Crystals* (Academic, New York, 1970)
15. B. Henderson, G.S. Imbusch, *Optical Spectroscopy of Inorganic Solids* (Oxford University Press, Oxford, 1989)
16. J.S. Griffith, *The Theory of Transition Metal Ions* (Cambridge University Press, Cambridge, 1961)
17. S. Kumar, Exploration of structural, morphological and magnetic properties of transition metal doped SnO2 films grown using pulsed laser deposition. Vacuum **182**, 109725 (2020). https://doi.org/10.1016/j.vacuum.2020.109725
18. A. Glavic, M.J. Björck, Appl. Cryst. **55**, 1063 (2022)
19. R. Zhao, L. Wang, X. Miao, L. Sun, W. Hua, Y. Wang, „Amino-capped zinc oxide modified Tin oxide electron transport layer for efficient perovskite solar cells. Cell. Rep. Phys. Sci. **2**, 100590 (2021). https://doi.org/10.1016/j.xcrp.2021.100590
20. A. Jorgetto, M.V. Boldrin Zanoni, M.O. Orlandi, Assessment of the superior photocatalytic properties of Sn^{2+}-containing SnO_2 microrods on the photodegradation of methyl orange. Sci. Rep. **13**, 14774 (2023). https://doi.org/10.1038/s41598-023-40659-8
21. W. Xia, H. Wang, X. Zeng, J. Han, J. Zhu, M. Zhou, S. Wu, High-efficiency photocatalytic activity of type II SnO/Sn_3O_4 heterostructures *via* interfacial charge transfer. Cryst. Eng. Comm. **16**, 6841 (2014). https://doi.org/10.1039/c4ce00884g
22. Zhang J., Lu J., Hu P., Lu P., Jia L, Yang Z., Preparation of ordered nanoporous WO3 thin films and the mechanism of large room-temperature ferromagnetism, Journal of the European Ceramic Society 43, 7533 (2023),https://doi.org/10.1016/j.jeurceramsoc.2023.08.023
23. Y.O. Kvashnin, O. Grånäs, Di I. Marco, M.I. Katsnelson, A.I. Lichtenstein, O. Eriksson, Exchange parameters of strongly correlated materials: extraction from spin-polarized density functional theory plus dynamical mean-field theory. Phys. Rev. B**91**, 125133 (2015).https://doi.org/10.1103/PhysRevB.91.125133